

# Growth of ZnO(0001) on GaN(0001)/4H-SiC buffer layers by plasma-assisted hybrid molecular beam epitaxy

David Adolph\*, Tobias Tingberg, Tommy Ive

Department of Microtechnology and Nanoscience (MC2), Chalmers University of Technology, 41296 Göteborg, Sweden



## ARTICLE INFO

### Article history:

Received 16 January 2015

Received in revised form

23 May 2015

Accepted 26 May 2015

Communicated by E. Calleja

Available online 6 June 2015

### Keywords:

A2. Single crystal growth

A3. Molecular beam epitaxy

B1. Gallium nitride

B1. Nitrides

B1. Oxides

B1. Zinc oxide

## ABSTRACT

Plasma-assisted molecular beam epitaxy was used to grow ZnO(0001) layers on GaN(0001)/4H-SiC buffer layers deposited in the same growth chamber equipped with both N- and O-plasma sources. The GaN buffer layers were grown immediately before initiating the growth of ZnO. Using a substrate temperature of 445 °C and an O<sub>2</sub> flow rate of 2.5 standard cubic centimeters per minute, we obtained ZnO layers with statistically smooth surfaces having a root-mean-square roughness of 0.3 nm and a peak-to-valley distance of 3 nm as revealed by atomic force microscopy. The full-width-at-half-maximum for x-ray rocking curves obtained across the ZnO(0002) and ZnO(10  $\bar{1}$  5) reflections was 198 and 948 arcsec, respectively. These values indicated that the mosaicity of the ZnO layer was comparable to the corresponding values of the underlying GaN buffer layer. Reciprocal space maps showed that the in-plane relaxation of the GaN and ZnO layers was 82% and 73%, respectively, and that the relaxation occurred abruptly during the growth. Room-temperature Hall-effect measurements revealed that the layers were inherently n-type and had an electron concentration of  $1 \times 10^{19} \text{ cm}^{-3}$  and a Hall mobility of  $51 \text{ cm}^2/\text{V s}$ .

© 2015 Elsevier B.V. All rights reserved.

## 1. Introduction

ZnO is interesting as a transparent contact to InGaN/GaN blue-violet light-emitting diodes (LEDs) [1] and other optoelectronic devices such as solar cells [2] or displays [3] or for the fabrication of hybrid ZnO/GaN LED structures [4]. ZnO has a wide and direct bandgap of 3.37 eV and is thus transparent into the near-ultraviolet (UV) region of the spectrum. Both ZnO and GaN crystallize in the wurtzite structure with similar in- and out-of-plane lattice constants  $a$  and  $c$ . For bulk ZnO,  $a_{\text{ZnO}} = 0.325$  and  $c_{\text{ZnO}} = 0.521$  nm, respectively, compared to  $a_{\text{GaN}} = 0.319$  and  $c_{\text{GaN}} = 0.518$  nm for GaN. The resulting ZnO/GaN lattice mismatch  $(a_{\text{ZnO}} - a_{\text{GaN}})/a_{\text{GaN}}$  is 1.9% which is a comparably small value. ZnO is also much cheaper and essentially non-toxic compared to the widely used indium-tin-oxide (ITO) transparent contacts. Furthermore, it is possible to obtain high-quality n-ZnO at a relatively low growth temperature. This is important for high-In containing InGaN compounds used for blue-green LEDs since a high growth temperature may adversely affect the quality of the InGaN layer. Both ZnO transparent contacts [1] and various hybrid ZnO/GaN LED structures have been demonstrated [4–7]. All these hybrid

structures were grown with the help of two different deposition systems. The InGaN/GaN layers were first grown in an epitaxy system dedicated for nitrides before the sample was removed and re-mounted in another system dedicated for the overgrowth of ZnO. Very often, metalorganic chemical vapor deposition (MOCVD) was used for the growth of InGaN/GaN while a range of techniques such as MOCVD, pulsed laser deposition (PLD) and molecular beam epitaxy (MBE) were used for the deposition of ZnO. The InGaN/GaN structures were thus exposed to air in this process which unavoidably resulted in the formation of Ga<sub>x</sub>O<sub>y</sub> sub-oxides on the nitride surface. These sub-oxides are detrimental to the structural quality of the overgrown ZnO layer and also the interface homogeneity of the ZnO/GaN interface [8–13]. The sub-oxides could also introduce a high density of non-radiative recombination centers [5]. The formation and thus the adverse effects of the sub-oxides can be avoided or minimized if the InGaN or GaN is not exposed to air before the growth of ZnO. This can be achieved with a combined nitride and oxide MBE-system where the same MBE growth chamber is used for both ZnO and GaN growth. We could find only one report on the growth of ZnO and GaN in the same MBE growth chamber despite the advantages with using such a system [14]. We have recently studied the effects of the sub-oxides using such a system [15].

In this work, we have investigated the structural, morphological and electrical properties of ZnO(0001) layers grown on GaN/

\* Corresponding author. Tel.: +46 317723327.

E-mail address: [adolph@chalmers.se](mailto:adolph@chalmers.se) (D. Adolph).

4H-SiC(0001) buffer layers by plasma-assisted MBE. Both ZnO and GaN were grown in the same MBE growth chamber. Our aim was to achieve layers with a smooth surface morphology and a high structural quality optimized for future hybrid ZnO/GaN applications such as LEDs. The samples exhibiting both a smooth surface morphology and a high structural quality were grown with a high O/Zn-ratio, a low growth rate, a low Zn-flux and with a high oxygen flow rate  $\Phi_{O_2}$ . We obtained ZnO films with a root-mean-square (RMS) roughness of 0.3 nm and a peak-to-valley (PV) distance of 3 nm as revealed by atomic force microscopy (AFM). The x-ray diffraction (XRD) rocking curve full-width-at-half-maximum (FWHM) of the ZnO(0002) and ZnO(10 $\bar{1}$ 5) reflections were 198 and 948 arcsec, respectively. Both surface morphology and rocking curve width were comparable to the corresponding values of the GaN buffer layers. Room-temperature Hall-effect measurements revealed that the ZnO layers exhibited a background electron concentration of  $1 \times 10^{19} \text{ cm}^{-3}$ . The Hall mobility  $\mu$  was  $51 \text{ cm}^2/\text{V s}$ .

2. Experiment

The growth experiments were conducted in a three-chamber MBE system equipped with solid source effusion cells for the evaporation of 6N Zn and 7N Ga and two VEECO radio-frequency (RF) plasma sources for the provision of active N and O, respectively. We used 7N N<sub>2</sub> and 6N O<sub>2</sub> gas for the respective plasma source. A reflectance high-energy electron diffraction (RHEED) system with an electron gun operated at 9.5 keV was used for monitoring the growth front. The MBE growth chamber base pressure was  $5 \times 10^{-10}$  Torr and the pressure during the growths was  $0.8\text{--}5 \times 10^{-5}$  Torr. All samples were rotated continuously during the growth experiments.

Three-inch unintentionally doped (n-type) 4H-SiC(0001) wafers purchased from CREE and post-polished by NovaSiC were used as substrates. The electrical properties were determined from ZnO layers grown on semi-insulating GaN/Al<sub>2</sub>O<sub>3</sub>-templates, with a sheet resistance  $R_s$  of 10 M  $\Omega/\square$ , from St. Gobain Crystals. All wafers were cleaved into  $1 \times 1 \text{ cm}^2$  pieces and sonicated in acetone, isopropanol and de-ionized water before they were mounted with In on the substrate holder. An in situ Ga-polishing or Ga flash-off procedure was performed prior to the GaN growth to remove sub-oxides residing on the SiC substrate surface [16]. This procedure also served as an independent temperature calibration.

The GaN buffer layers were grown on the 4H-SiC substrates at 700 °C under Ga-stable conditions [16]. The sample rotation was 6 rpm during all growths. All buffer layers were 100–200 nm thick. After terminating the GaN buffer layer growth, the substrate temperature  $T_s$  was decreased to 300–550 °C. The N-plasma source was switched off between 500 and 550 °C. A 1–3.5 min pre-deposition of metallic Zn on the GaN buffer layer was performed before the O-plasma source ignition which initiated the ZnO growth. The O-plasma source was operated at 300 W for all growths.

The surface morphology was examined with an Ultra 55 FEG scanning electron microscope (SEM) and a Bruker Dimension 3100 AFM operated in tapping mode with a Si cantilever. The layer thickness was verified from cross-sectional SEM micrographs of the cleaved sample edge. The growth rate was calculated by dividing the measured thickness with the growth time. The Zn-deposition rate was calibrated by Zn-deposition, with a substrate at room temperature, followed by thickness determination with SEM. X-ray diffraction (XRD) using a Panalytical X'Pert PRO MRD four-circle triple-axis diffractometer equipped with a Cu $\text{K}\alpha_1$  source in the focus of a Ge(220) hybrid monochromator was employed to

analyze the structural quality. The mosaicity (tilt and twist) of the layers was examined by recording x-ray rocking curves (XRCs) across the on-axis symmetric (0002) reflection and across the (10 $\bar{1}$ 5) reflection (in skew-symmetric geometry), respectively. Reciprocal space maps (RSMs) were obtained for the off-axis (10 $\bar{1}$ 5) reflection to determine the in-plane relaxation of the ZnO and GaN layers. A HL5500 Hall room temperature measurement setup was used for the electrical characterization.

The ZnO(0001) polarity was determined with etch experiments. An etch time of 10 s in a 0.012 M HCl solution showed hexagonal pits, verified with SEM micrographs, on the ZnO-surface characteristic for a Zn-face layer [17].

3. Results and discussion

The growth conditions and the morphological and structural properties for a representative set of samples presented in this work are summarized in Table 1.

Fig. 1 shows the RHEED patterns for the [11 $\bar{2}$ 0] azimuth from ZnO layers grown on GaN/4H-SiC at the end of the growth. The vaporization temperature of Zn is 200–205 °C at the growth

**Table 1**  
Summary of the growth conditions and selected properties for a representative set of samples presented in this work. Listed is the growth temperature  $T_s$ , the Zn-flux, the O<sub>2</sub> flow rate  $\Phi_{O_2}$ , the layer thickness  $d$ , the RMS roughness and PV distance as determined from AFM scans over  $2 \times 2 \mu\text{m}^2$  and the FWHM of XRCs across the (0002) and (10 $\bar{1}$ 5) reflections, respectively.

Sample	$T_s$ (°C)	Zn-flux (Å/s)	$\Phi_{O_2}$ (sccm)	$d$ (nm)	RMS (nm)	PV (nm)	$\Delta\omega(0002)$ (arcsec)	$\Delta\omega(10\bar{1}5)$ (arcsec)
A	440	1.4	2.0	80	0.8	6.5	198	948
B	445	1.4	2.5	50	0.34	3.3	294	1150
C	440	1.4	3.0	34	0.47	4.8	–	–
D	445	1.4	1.5	43	0.70	6.2	319	1228
E	440	1.4	1.0	57	0.98	9.9	380	1078
F	440	1.3	2.0	34	0.26	3.7	–	–
G	450	8.5	2.0	155	9.3	73	405	1014
H	440	2.1	2.0	144	4.6	36	355	985
I	295	8.5	2.0	260	11.6	107	637	1327
J	500	2.7	2.0	80	3.4	3.0	533	2218

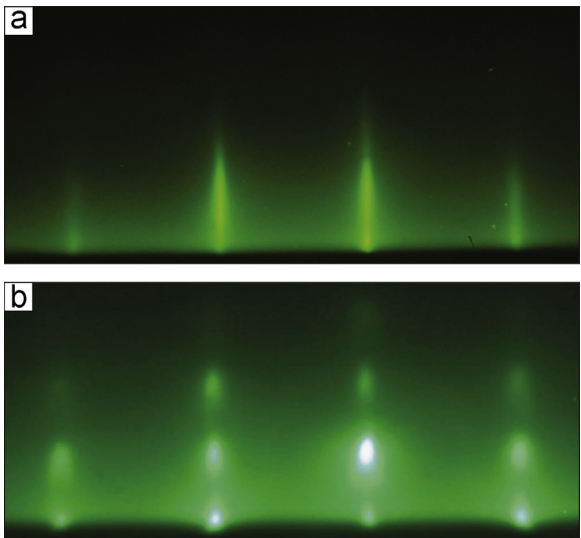


**Fig. 1.** (a) End-of-growth RHEED pattern for the [11 $\bar{2}$ 0] azimuth from a ZnO/GaN/4H-SiC sample grown with a Zn-flux 1.4 Å/s and  $\Phi_{O_2} = 2.0$  sccm at  $T_s = 440$  °C (sample A in Table 1). (b) RHEED pattern from a sample grown with a lower O/Zn-ratio.

Download English Version:

<https://daneshyari.com/en/article/1789889>

Download Persian Version:

<https://daneshyari.com/article/1789889>

[Daneshyari.com](https://daneshyari.com)